International Journal of Green Energy

ISSN: 1543-5075 (Print) 1543-5083 (Online) Journal homepage: http://www.tandfonline.com/loi/ljge20

Analysis of a solar photovoltaic-assisted absorption refrigeration system for domestic air conditioning

A. Ganguly & Dipankar N. Basu

To cite this article: A. Ganguly & Dipankar N. Basu (2016) Analysis of a solar photovoltaic-assisted absorption refrigeration system for domestic air conditioning, International Journal of Green Energy, 13:6, 585-594, DOI: 10.1080/15435075.2014.977442

To link to this article: http://dx.doi.org/10.1080/15435075.2014.977442

INTERNATIONAL JOURNAL OF GREEN ENERGY, 2016
VOL. 13, NO. 6, 585–594
http://dx.doi.org/10.1080/15435075.2014.977442

Taylor & Francis
Taylor & Francis Group

Analysis of a solar photovoltaic-assisted absorption refrigeration system for domestic air conditioning

A. Ganguly[a] and Dipankar N. Basu[b]

[a]Department of Mechanical Engineering, Indian Institute of Engineering Science and Technology, Shibpur, Howrah, India; [b]Department of Mechanical Engineering, Indian Institute of Technology Guwahati, Guwahati, India

ABSTRACT

Theoretical model of a solar photovoltaic integrated water-Lithium bromide absorption system is presented for domestic air conditioning. Surplus electrical energy from photovoltaic modules is used for charging the battery, which is utilized during the periods of zero or insufficient solar radiation. Minimum solar area required for each month is calculated and October is identified as the month requiring the highest area of photovoltaic arrays for a constant cooling load of 3.5 kW. The integrated system is found to be capable of sufficient amount of surplus electrical energy generation during both summer and winter months, with a daily excess of about 815 Ah of electrical energy on average over a complete calendar year. Designed system is found to be economically viable, having an energy payback period of 2.7 years.

KEYWORDS

Absorption refrigeration; solar photovoltaics; air conditioning; cost analysis; climatic cycle

Introduction

Refrigeration and air conditioning has become an active area of research in view of the present global concern towards energy conservation and environment protection. Commonly used synthetic refrigerants in traditional vapor compression refrigeration systems are not nature-friendly, while the knowledge base about alternative technologies such as supercritical CO_2 system, vortex tube, and magnetic refrigerator is still under development. In this context, the vapor absorption refrigeration system (VARS) can become popular particularly for large-scale applications. Most attractive feature of VARS is the utilization of low-grade thermal energy for its operation (Arora 2007) and thus it exhibits a huge potential for saving primary energy sources, while reducing environmental encroachment. However, lower COP is generally the major limitation of any VARS. So, to make it viable, VARS needs to be coupled with an easily accessible source of low-grade heat and this opens up a very prospective area of utilization of solar energy (Best and Ortega 1999; Zhai and Wang 2009). Sustained effort to use solar energy for achieving low temperature is underway for last couple of decades. However, its application in powering refrigeration systems is still very limited.

Kim and Ferreira (2008) compared different designs of solar electric and solar thermal systems. Single-effect Water–Lithium bromide (H_2O–LiBr) absorption system was found to be the most feasible one. Asdrubali and Grignaffini (2005) experimentally evaluated the performance of single-effect H_2O–LiBr system and showed that it can perform admirably with optimum hot water supply temperature of around 65–70°C. Pongtornkulpanich et al. (2008) developed a solar-driven 10 TR H_2O–LiBr system in association with an evacuated tube solar collector. Their analysis showed that the economics of the cooling system were dominated by the initial investment and about 19% of required thermal energy was needed to be supplied from LPG-fired backup heating unit. This particular fact is generally the prime concern of solar thermal-based coolers, as the prevalent options of thermal energy storage are not economical, often requiring the use of auxiliary energy source during zero-insolation periods.

The advancement in solar photovoltaic technology over the years has offered an alternative option of developing a multi-objective system. Tiwari, Mishra, and Solanki (2011) reviewed the PV and hybrid PV-thermal systems working with water and air as working fluids. Their promising features were emphasized and lots of scope for improvement, particularly for roof-top installation, was highlighted. Kumar and Rosen (2011), however, suggested further research before adoption of hybrid collectors. Classical PV systems are well-explored though, as Razykov et al. (2011) reported an annual market growth rate of 35–40% for mono- and poly-crystalline thin-film PV technology. Such development, along with increased practical efficiencies, has resulted in substantial reduction in the cost of solar cells. Hence, incorporation of solar PV-modules for energizing an absorption system is very much practicable, from the view point of both system operation and recovery of capital investment. It is a common observation about absorption chillers that the highest system COP is obtained around some specific generator temperature (Marcos, Izquierdo, Palacios 2011). Energy input to the generator through a resistance heater allows better control of the generator temperature, as well as easy quantification of the

CONTACT Dipankar N. Basu dipankar.n.basu@gmail.com Department of Mechanical Engineering, Indian Institute of Technology Guwahati, Guwahati, Assam 781039, India.

amount of energy to be supplied. Also, the same is easily available, highly reliable, and has point of use service. Electrical energy developed from solar PV cells can be stored easily for utilization during zero-insolation periods. That also allows utilization of surplus electrical energy for other purposes, such as running system auxiliaries or illuminating the conditioned space, etc. Besides, if the objective is to develop a stand-alone solar refrigeration system, incorporation of solar photovoltaic modules is the more feasible option compared to that of solar thermal. However, such type of integration effort is very scarce in literature. Enibe (1997) introduced photovoltaic-powered vapor compression systems as well as continuous and intermittent liquid or solid absorption and adsorption systems as possible alternatives. Chen and Hihara (1999) modeled an absorption cycle co-driven by solar energy and electricity. Their results showed that the new cycle successfully surmounted certain shortcomings of the traditional absorption cycle with unsteady energy input from a variable source. The system also exhibited increased system COP. Mastrullo and Renno (2010) studied a heat pump whose evaporator was operated as a photovoltaic collector, thereby realizing a comparison with traditional heat pump. However, none of such studies converged towards providing a practicable solution. Recent experimental work of Chien et al. (2013) is probably the first effort of integrating solar photovoltaic system to VARS for transportation applications and for remote locations. A NH_3–H_2O system with about 65 W cooling capacity was demonstrated with a solar cell area of 1.78 m^2. The system was able to maintain temperature of 5–8°C after 160 min of operation, thereby encouraging a promising area of research.

As reported by Moharil and Kulkarni (2009), there are 94,000 un-electrified villages in India, of which 25,000 villages are located in such remote areas that the extension of the existing electricity grid there is not economically viable. In distant future, even if those places get connected to power grid, there will be problems like low voltage, high power fluctuation, and frequent breakdowns, along with abnormally large transmission and distribution losses. Use of conventional grid-connected refrigeration or air conditioning system is impossible in such locations. Compression-based systems require large starting current and also exhibit poor part-load performance, needing additional powering option, which can be redundant during normal run and hence are not the best option to couple with renewable energy sources. Present work, therefore, conceptualizes the option of incorporating solar photovoltaic modules for powering air-cooled H_2O–LiBr absorption system for domestic air conditioning and also for co-generation of electricity. A mathematical model for the same has been developed, which comprises of the absorption chiller, PV modules, and the storage battery. Electrical energy required for the absorption system is in the form of heating load to the generator and direct electrical input to the solution pump and cooling fan. PV modules generate electricity during the sunshine periods. If the photovoltaic generation is higher than the requirement for the absorption system, the surplus energy is utilized for charging the battery. During periods of insufficient or zero solar insolation, battery provides the necessary backup of electrical energy. The associated power system decides the direction of current flow in or out of the battery. Schematic

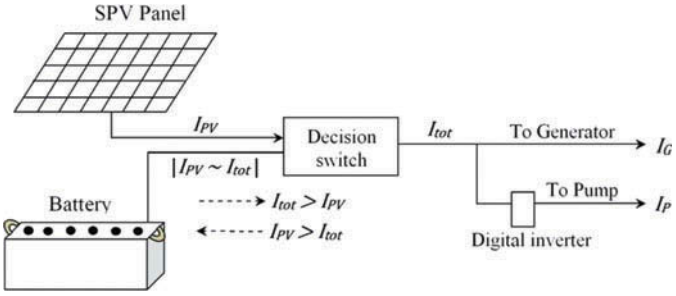

Figure 1. Schematic representation of the photovoltaic-powered absorption system.

representation of the complete scheme of integrated operation is shown in Figure 1. Real climatic data for Kolkata, India (22.39° N, 88.27° E), is utilized for analyzing the performance of the system over a complete calendar year. Finally, a cost analysis is performed to estimate the unit cost of electrical energy for operation of such a system along with the payback period.

Theoretical model development

A schematic representation of a single-stage vapor absorption refrigeration system is shown in Figure 2. The evaporator is subjected to a cooling load of $\dot{Q}_E$, whereas $\dot{Q}_G$is the heat input to the generator through a DC electrical heater. The solution stream leaving the absorber is denoted as the *strong solution*, whereas the returning solution is identified as the *weak solution*. The heat exchanger incorporated in the refrigerant-side helps to recover a part of the energy from the weak solution, thereby improving the COP of the system.

Assumptions

Following simplifying assumptions have been made while formulating the theoretical model of the absorption system.

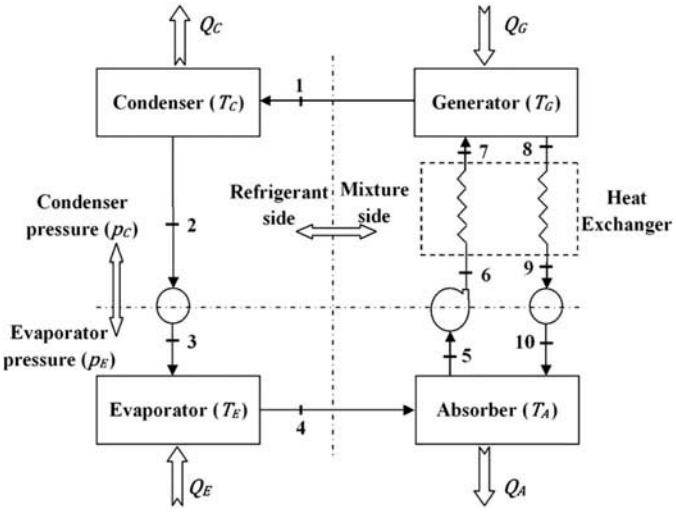

Figure 2. Schematic representation of single-stage vapour absorption refrigeration system.

(i) System is under steady-state condition, with no frictional losses inside the pipings.
(ii) Refrigerant leaves the condenser in the form of saturated liquid and leaves the evaporator as dry saturated vapor.
(iii) Solutions leaving the generator and the absorber are saturated mixtures corresponding to their respective temperatures.
(iv) Both refrigerant and solution valves are isenthalpic.
(v) All the components are ideally insulated from the surroundings.

Analysis of absorption refrigeration system

Analysis of the absorption system comprises of carrying out mass balance and energy balance across each of the system components. Energy balance across the evaporator yields

$$\dot{Q}_E = m_r(h_4 - h_3) \tag{1}$$

Similarly mass balance of LiBr and overall mass balance across the absorber gives

$$X_{ss}\dot{m}_{ss} = X_{ws}\dot{m}_{ws}, \tag{2}$$
$$\dot{m}_{ss} = \dot{m}_r + \dot{m}_{ws}. \tag{3}$$

Accordingly, the mass flow rate for strong and weak solutions can be estimated as

$$\dot{m}_{ss} = \frac{X_{ws}}{X_{ws} - X_{ss}}\dot{m}_r, \tag{4}$$

$$\dot{m}_{ws} = \frac{X_{ss}}{X_{ws} - X_{ss}}\dot{m}_r. \tag{5}$$

Absorber heat rejection can be calculated using energy balance across the component as

$$\dot{m}_r h_4 + \dot{m}_{ws}h_{10} = \dot{Q}_A + \dot{m}_{ss}h_5. \tag{6}$$

Similarly, the energy balance across the generator yields generator heat load as

$$\dot{Q}_G + \dot{m}_{ss}h_7 = \dot{m}_r h_1 + \dot{m}_{ws}h_8. \tag{7}$$

Heat exchanger effectiveness is defined as

$$\epsilon = \frac{h_8 - h_9}{h_8 - h_6} \approx \frac{T_G - T_9}{T_G - T_6}. \tag{8}$$

External energy requirement for the pump can be calculated as

$$\dot{W}_P = \frac{\dot{m}_{ss}}{\eta_P}(h_6 - h_5) = \frac{\dot{m}_{ss}}{\eta_P}\int_{p_E}^{p_C} v\,dp. \tag{9}$$

Here, η_P represents the pump efficiency. The pump is expected to operate with varying solution flow rates and hence adjustable speed drive is considered for energy saving. However, the energy consumed by the pump is generally negligibly small and hence choice of pump characteristics hardly has any effect on overall performance prediction. Pressure drop across the cooling fan (Δp_F) is calculated following Lin, Wang, and Xia (2011) as

$$\Delta p_F = 1.76u_F^{1.6312}n. \tag{10}$$

In Eq. (10), n refers to the number of rows in the absorber and u_F is the air velocity through the fan. Same parameter values for the fan are considered as used by Lin, Wang, and Xia (2011). Accordingly, the power consumed by the fan can be given by

$$\dot{W}_F = \dot{V}_{air}\,\Delta p_F/\eta_F. \tag{11}$$

Finally, the system COP can be represented as

$$COP = \frac{\dot{Q}_E}{\dot{Q}_G + \left(\dot{W}_P + \dot{W}_F\right)}. \tag{12}$$

Here, the properties of H_2O–LiBr solution are estimated following the correlations presented by Patek and Klomfar (2006), whereas pure refrigerant properties are calculated following the IAPWS-IF97 formulation (Wagner et al. 2000). Heat exchanger effectiveness (ϵ) is assumed to be 0.85 throughout the study, while the pump efficiency (η_P) is considered to be 0.9.

Modeling of SPV-Based power system

Photovoltaic modules are devices that convert the solar radiation directly into electricity and hence the output electrical energy is directly a function of the solar radiation intensity. It is a common practice (Kim and Ferreira 2008) to consider an efficiency factor of the module, which gives the output energy as

$$\dot{E}_{PV} = \eta_{PV}GA. \tag{13}$$

Here, A refers to the available area of the photovoltaic array, which is a combination of a number of modules connected in series and parallel to achieve the desired output voltage and current. Number of modules connected in series (N_s) in an array depends on the output voltage required for the selected operation and can be given by

$$N_s = \frac{V_{\text{system}}}{V_t}. \tag{14}$$

In the present work, the system voltage (V_{system}) is considered to be 36 V, same as that of the module terminal voltage (V_t). Hence, one module is needed in each arm of the photovoltaic array. Number of modules to be connected in parallel is governed by the design current requirement from the power system, which must be capable of supplying the electrical energy required by the absorption system throughout the day. The design current requirement can be estimated as

$$I_{PV,des} = \frac{J_{tot} \times DF}{\text{Peak Sunshine Hours} \times \eta_{cc}}. \tag{15}$$

Here, the module de-rating factor (DF) and efficiency of charge controller (η_{cc}) are considered to be 1.25 (TEC 2004) and 0.85, respectively. The duration of peak sunshine period is assumed to be 7 hr, considering the location to be Kolkata situated in the Gangetic plains of eastern India (Patra and Datta 2003). Electrical energy needed by the absorption system is in the form of direct current to the resistance heater in generator and alternating current to the motors of solution

pump and cooling fan. Both the photovoltaic generation and storage battery discharge being in the form of direct current, DC-to-AC conversion through a digital inverter is necessary for pump and fan operation, while direct supply can be provided to the generator. Hence, the total electrical energy requirement for the absorption system for a representative day can be given by

$$J_{\text{tot}} = \frac{1}{V_{\text{system}}} \sum_{OH} \left\{ \frac{\dot{Q}_G}{\eta_{\text{wire}}} + \frac{\left(\dot{W}_P + \dot{W}_F\right)}{PF\left(\eta_{inv} \times \eta_{\text{wire}}\right)} \right\}. \tag{16}$$

In Eq. (16), *OH* represents the number of operating hours in a typical day. Inverter and wire efficiencies are considered to be 0.90 and 0.98, respectively, while the system power factor (*PF*) is assumed to be 0.85. Thus, the number of PV modules to be connected in parallel can be estimated as

$$N_p = \frac{I_{PV,\text{des}}}{I_{\text{mpp}}}. \tag{17}$$

Here, I_{mpp} is the current available from a single PV module under peak power condition. Thus, knowing the number of modules in parallel in the photovoltaic array, the PV generation of the system can be determined on an hourly basis.

Sizing of storage battery

Battery is an important component in the power system design. In the present system, the battery provides the necessary backup of electrical energy and caters to the same to the absorption system whenever the PV generation is insufficient compared to the demand. In the present work, the sizing of the battery is done following the guidelines of TEC, India (2004). Considering an expected battery capacity of 120% with 2 days of autonomy and a permissible Depth-Of-Discharge of 80% under normal working temperatures, the battery capacity can be given by

$$J_{\text{battery}} = 2.0833(\text{load per day}). \tag{18}$$

Daily load for battery sizing analysis has been considered as the amount of electrical energy to be supplied by the battery during zero or insufficient solar radiation periods. Such load varies widely over different seasons and also depends on the operation schedule in various months. So the highest value over a calendar year is employed for estimating the storage capacity.

Numerical scheme of analysis

A computational model is developed for characterization of SPV-supported VARS unit by integrating the single-effect H_2O–LiBr absorption chiller and SPV-based power system. The absorption system is designed for a constant cooling load of 3.5 kW throughout the day with an evaporator temperature of 15°C, while the generator temperature is kept constant at 80°C. The condenser and absorber temperatures, however, vary depending on the temperature of supplied coolant stream, which is a function of the instantaneous ambient condition. Therefore, in the present work, condenser and absorber temperatures at any instant are assumed to be 5°C more than the prevailing ambient temperature. Monthly average values of ambient climatic data in the form of solar radiation, ambient temperature, and wind speed over 24 hr are provided as input to the theoretical model (Tiwari 2004). In order to avoid superfluous operation of the integrated system under cold condition, it is decided to cut-off the absorption unit when the ambient temperature falls below 20°C.

Numerical calculations are performed over a complete calendar year and area of solar array required to meet the demand over various months is calculated. Central Electronics Limited (CEL) make PM-150 (CEL 2011) is selected as the target module. Accordingly, the number of solar modules required to form the array and the minimum battery capacity requirement are calculated. Considering the needs for all the months, it is decided to have 65 modules of PM-150 connected in parallel within the solar photovoltaic array. A battery bank having storage capacity of 1,600 Ah (8×200 Ah) is found to be satisfactory.

Economic analysis

It is also important to have a rudimentary estimate about the possible cost involved in running such a system in order to check its financial viability. The procedure detailed by Chel, Tiwari, and Chandra (2009) is followed here. The most important component of the power system is definitely the PV modules, the cost of which can be estimated as

$$C_{PV} = N_p \dot{E}_{\text{peak}} \times \text{cost per unit peak power}. \tag{19}$$

Here, $\dot{E}_{\text{peak}}$ is the peak power output from each module. In the present work, the cost per unit peak power is considered to be US$4.85 (Chel, Tiwari, Chandra 2009). The cost of battery bank is determined based on its actual capacity and can be given by

$$C_{\text{battery}} = J_{\text{battery}} \times \text{Cost per Ah}. \tag{20}$$

The power conditioning unit consists of the charge controller and the inverter. Cost of the charge controller can be estimated as

$$C_{cc} = \frac{N_p \dot{E}_{\text{peak}}}{V_{\text{system}}} \times \text{cost per } A. \tag{21}$$

Similarly, the cost of the inverter is given as

$$C_{\text{inverter}} = \left(1.1 \times \dot{E}_{\text{peak}}\right) \times \text{cost per} W. \tag{22}$$

Here, the unit costs are taken as US$1/Ah for the battery, $5.87/A for the charge controller, and $0.719/W for the inverter (Chel, Tiwari, Chandra 2009). Complete power system in present analysis has been considered to be building integrated and hence the cost of the balance of the system can be neglected, along with the salvage or scrap value (Chel, Tiwari, Chandra 2009). Accordingly, the initial investment for the power system can be represented as

$$C_{\text{in}} = C_{PV} + C_{\text{battery}} + (C_{cc} + C_{\text{inverter}}). \tag{23}$$

Life-cycle analysis for the system is carried out assuming the useful life for the PV array to be 30 years and the same for

battery bank to be 5 years. The old batteries can be replaced after every 5 years with an assumed rebate of 7% on total cost of the new battery bank in a country like India and so the replaced battery bank will cost 0.93 times C_{battery}, assuming the cost of battery bank remains uniform throughout the life of the PV array. Accordingly, the present battery bank cost can be estimated as

$$C_B{}' = 0.93 \times C_{\text{battery}}\left[\frac{1}{(1+i)^5}+\frac{1}{(1+i)^{10}}+\frac{1}{(1+i)^{15}}+\frac{1}{(1+i)^{20}}+\frac{1}{(1+i)^{25}}\right]. \quad (24)$$

Finally, the uniform annualized cost of power system (C_{ann}) can be given by (Chel, Tiwari, Chandra 2009)

$$C_{\text{ann}} = (C_{in} + C_B{}')\left[\frac{i(1+i)^{30}}{(1+i)^{30}-1}\right]. \quad (25)$$

Here, the rate of interest (i) is selected to be 4%, which is offered by Government of India to promote the use of solar energy applications.

Considering the annual maintenance cost to be 10% of C_{ann}, the annualized life cycle cost (ALCC) for the power system in USD per year is determined as

$$ALCC = 1.1 \times C_{\text{ann}}. \quad (26)$$

This figure can be divided by the total annual electrical energy consumed by the absorption system in kWh to get the required value of cost per unit of electricity generated by the PV modules.

Estimation of energy payback period of a photovoltaic system requires knowledge of embodied energy from resource extraction through manufacturing, product use until the end of life span, as well as energy output from the system per year in kWh. It represents the time period after which the energy yield compensates the energy investments and can be calculated as Nawaz and Tiwari (2006)

$$\text{EPBT} = \text{Embodied energy } (\text{kWh/m}^2)/\text{Energy output } (\text{kWh/m}^2/\text{year}). \quad (27)$$

Total embodied energy at macro-level for a typical monocrystalline silicon PV module is 1,380 kWh/m^2.

Results and discussion

Three important variables characterizing the ambient climatic condition have been considered here, namely, solar radiation intensity, air temperature, and the wind speed. Kolkata being a densely populated city, wind speed is generally very low and its effect is also minimal. Ambient temperature however has significant effect, as evident from Figure 3. As the heat rejection in condenser ($\dot{Q}_C$) is dependent on the temperature of the cooling water, any change in ambient temperature results in corresponding change in the system COP. Any increase in condenser temperature and associated enhancement in its saturation pressure requires larger energy input to the mixture-side of the system. So, the heat input to the generator ($\dot{Q}_G$) increases, thereby lowering the COP of the system. Small

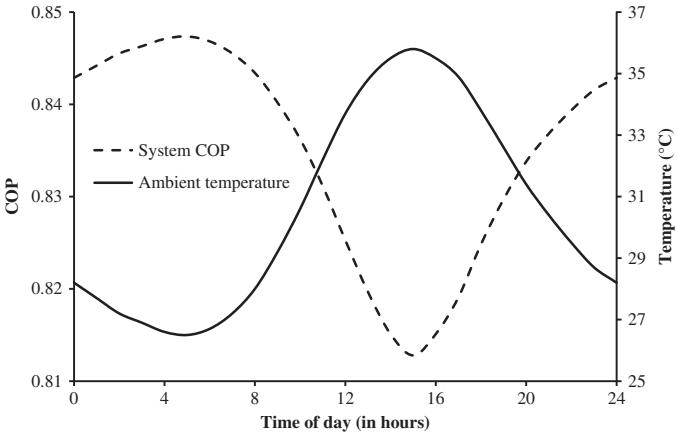

Figure 3. Hourly variations in system COP and ambient temperature over a representative day for the month of May.

augmentation in pump work can also be observed. The reverse is true for reduction in ambient temperature, which is clearly depicted in Figure 3. It is found that system COP and ambient temperature exhibits a 180° out-of-phase variation; the time for the lowest temperature perfectly matches with the highest COP point. A rise in ambient temperature by about 9.3°C between early morning and the late afternoon produces nearly 4.25% decline in the COP of the system. Energy input to the generator varies almost in-phase with the ambient temperature and about 4.32% increase has been observed in its value. Hourly variations of the solution flow rates have been shown in Figure 4 for the month of May, which is representative of the summer season in Kolkata. Both weak and strong solution flow rates vary considerably with time, the peak value closely matching the time of the day when the ambient temperature is the maximum. It is observed (from Figure 4) that the mass flow rate of the strong solution around 3 PM is more than three times of its value at around 5 AM. The mass flow rate of the weak solution essentially follows the same trend (as given by Eq. (3)). The generator load variation, being reciprocal of the system COP, also exhibits an identical profile. The solar radiation, however, does not have any significant effect on the COP of the system and

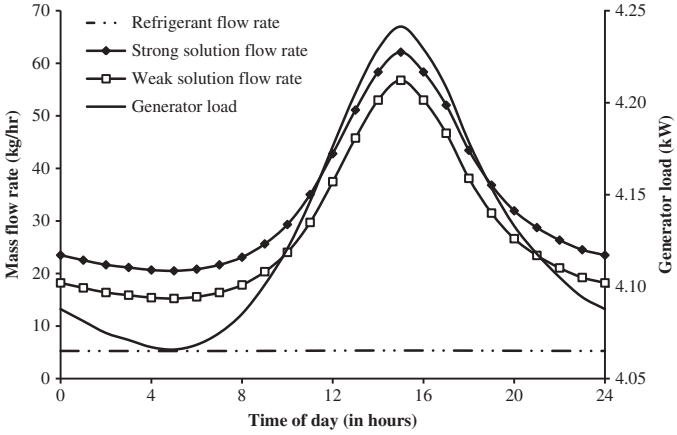

Figure 4. Hourly variations in refrigerant and solution flow rates and generator load over a representative day for the month of May.

the performance of the VARS can be considered to be invariant of the intensity of solar radiation.

In order to characterize the integrated system, it is essential to identify the required number of modules to be connected in parallel in the SPV-array. The amount of energy consumed by the absorption unit and the same produced by each SPV module are compared in Figure 5 for a representative day in the month of May. Cooling load being constant, electrical energy requirement changes only by a small amount (around 4.2%) over a typical day. Daylong ambient temperature remains well above 20°C in summer and hence the VARS unit is working all through 24 hr. SPV modules can produce energy only for certain hours and corresponding magnitude is maximum around 12 noon, as it closely corresponds to the hour of the highest solar radiation intensity. Energy produced by the SPV array must satisfy the cumulative requirement of the absorption unit throughout a calendar year. Hence, the minimum area required for each month has been computed considering 20% efficiency of solar cells (η_{PV}) and the same has been presented in Figure 6, along with the total electrical energy requirement for the concerned months. As the cooling load has been assumed to be constant, energy requirement remains nearly the same apart from the winter months (November to February), when the surrounding temperature falls below the specified cut-off value of 20°C. The magnitude of minimum area required, however, varies considerably due to the variation in available radiation level in different months. Peak summer and early monsoon months (April–July) provide ample radiation, allowing a lower area requirement. Very small area is required for the winter months owing to reduced system load. Post-monsoon period of October, however, provides a unique situation, where level of radiation is moderately low and the ambient temperature is sufficiently high, forcing all-day operation of the absorption unit. Accordingly, the highest solar requirement is obtained for the month of October and the concerned value in present design is found to be around 79.6 m^2. Despite the reduced load, reasonably large solar area is also required for November, due to the low radiation levels. Values of minimum solar area and corresponding number of PM-150 modules (1.58 m × 0.795 m) for a few selected months are given in Table 1. Keeping the obligation of October in view, it was decided to have 65 modules of PM-150 in parallel in the designed SPV-array.

In an effort to characterize the designed photovoltaic system, hourly variation in energy produced by the designed SPV array for representative days of various months are shown in Figure 7, while Figure 8 shows the variation of cumulative daylong energy production for representative days in various months of a full climatic cycle. Highest production for any particular hour, as well as the cumulative production, is maximum for the month of June and minimum for the month of January, which is very much expected. Rapid increase in available solar radiation intensity after the winter months is

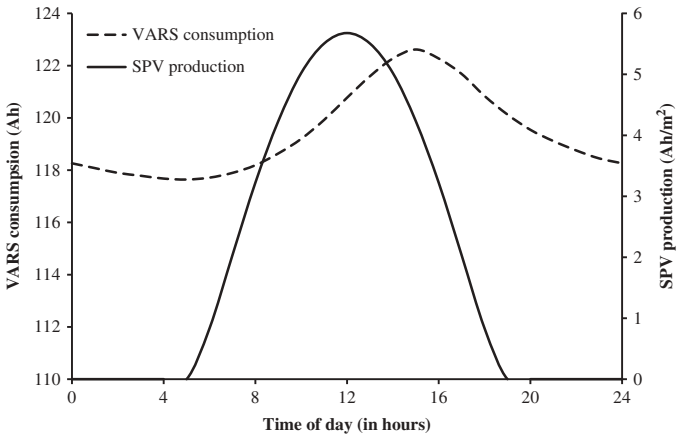

Figure 5. Hourly variations in electrical energy consumed by VARS unit and electrical energy produced per unit area of SPV module over a representative day for the month of May.

Table 1. Solar Area Requirement and Corresponding Number of PM-150 Modules for a Few Selected Months.

	Required solar area (m^2)	Number of PM-150 modules
January	37.383	30
March	68.834	55
June	57.785	47
September	69.172	56
October	79.598	64

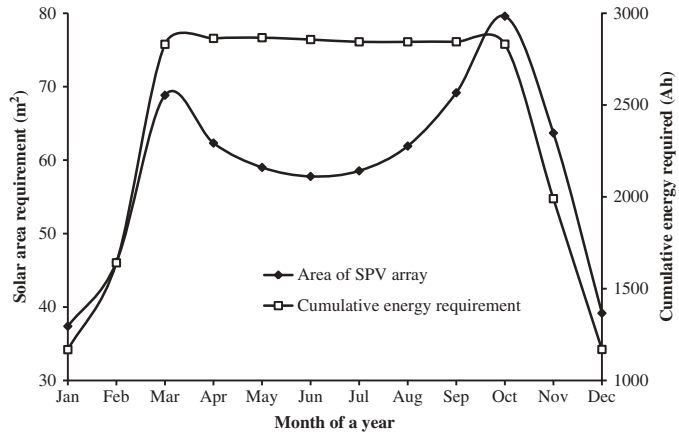

Figure 6. Month-wise variation in minimum area requirement for the SPV array and cumulative energy requirement.

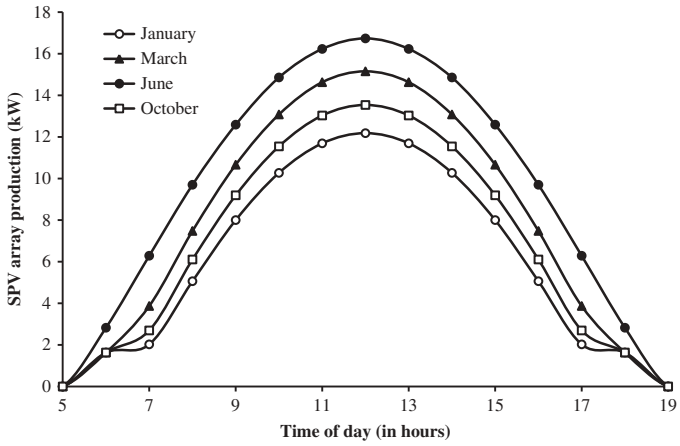

Figure 7. Month-wise variation in hourly energy production from the proposed SPV array over a typical day of each month.

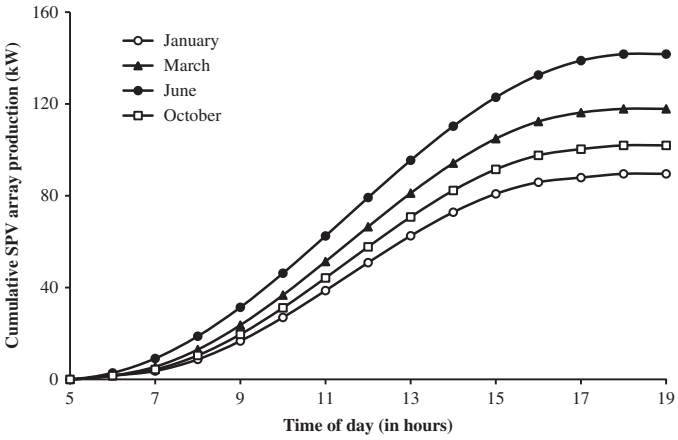

Figure 8. Month-wise variation in cumulative energy produced by the proposed SPV array over a typical day of each month.

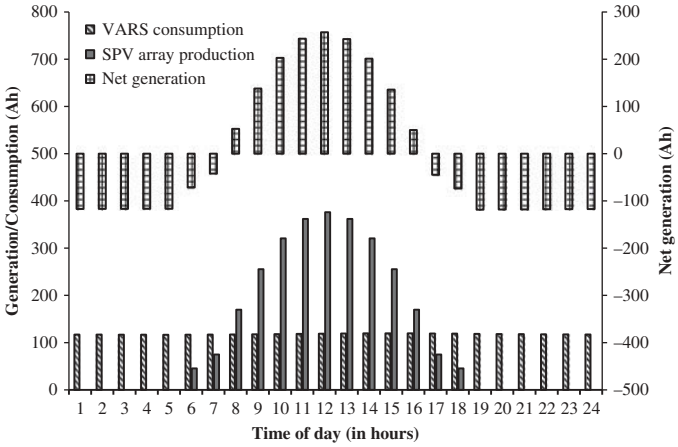

Figure 10. Hourly variation of electrical energy production and consumption by integrated system and net energy flow diagram for a representative day of October.

evident from the difference in electrical energy generation levels between January and March. But energy produced in October is only marginally higher than that in January, which necessitates large solar area requirements, as discussed earlier.

A comparison in cumulative energy consumption by VARS and production by SPV array for the month of October is presented in Figure 9. A near-linear profile can be observed for energy consumed by the absorption unit, whereas the SPV array starts to operate only after 5 AM and is active up to about 6 PM. The cumulative SPV production becomes higher than corresponding value of VARS consumption and provides sufficiently large amount of surplus energy only after 11 AM. But, as there is no photovoltaic generation beyond 6 PM, VARS operates by drawing energy from the storage battery. Both the quantities become nearly equal to each other by the end of the day. An energy flow diagram for the month of October is presented in Figure 10. Surplus energy is available only for 9 hr in a typical day, whereas deficit energy needs to be supplemented by the storage battery for the remaining hours. During early-morning (6–7 AM) and late-afternoon (5–6 PM), more energy is consumed by the absorption system than that produced from the SPV array. Still the surplus energy generated between 8 AM and 4 PM is adequate to cater to the need for the entire day.

Due to cold ambient conditions in the month of January, VARS starts to operate only after 10 AM and shuts down again at around 8 PM (Figure 11). The SPV array, however, produces sufficiently large amount of energy during the daytime, providing a significant gain in net energy production. The total photovoltaic generation is more than double of the energy consumed by the absorption unit, as evident from Figure 11. The same is further substantiated through the energy flow diagram shown in Figure 12. Only for 4 hr during the late-afternoon and during the evening (5–8 PM), battery needs to provide the energy back-up. Huge amount of surplus electrical energy is therefore available in the month of January and the same is true for other winter months.

Intensity of solar radiation considerably increases after the winter season, along with the ambient temperature. So full 24 hr operation becomes necessary and surplus energy is available only for 9 hr in a typical day (Figure 13), similar to October. However, SPV generation is much higher in March, with the peak hourly production being nearly 45 Ah higher than the same in October. Hence, net gain in electricity is quite appreciable. In the month of June (summer season in India), the photovoltaic generation is max-

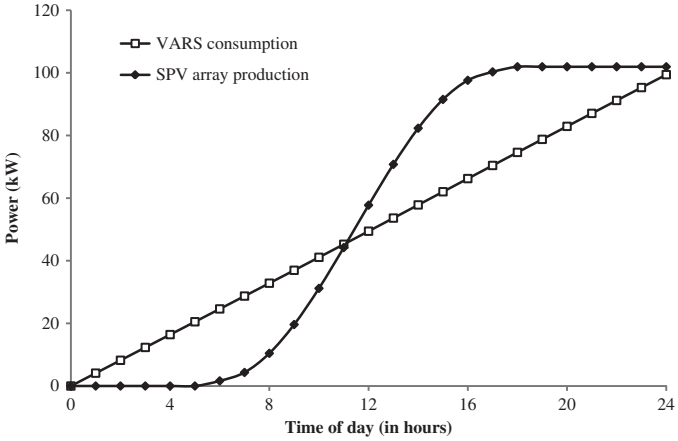

Figure 9. Hourly variation in cumulative power consumption by VARS and production by proposed VARS array in the month of October.

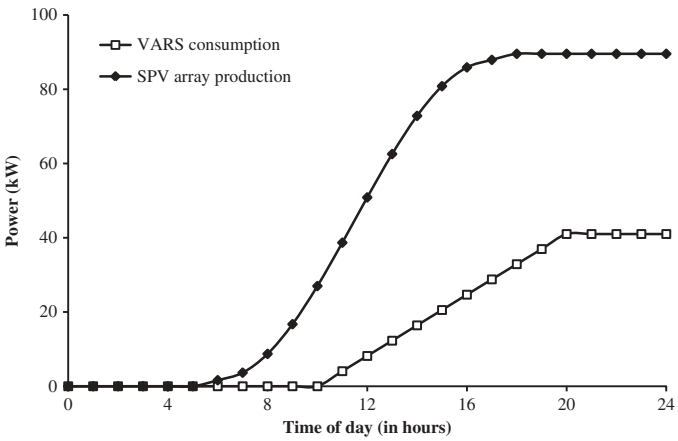

Figure 11. Hourly variation in cumulative power consumption by VARS and production by proposed VARS array in the month of January.

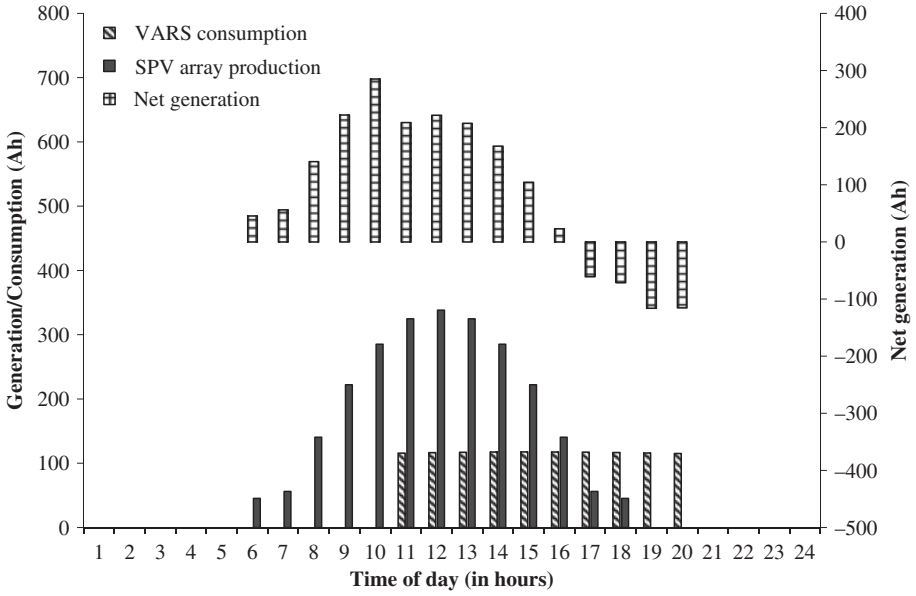

Figure 12. Hourly variation of electrical energy production and consumption by integrated system and net energy flow diagram for a representative day of January.

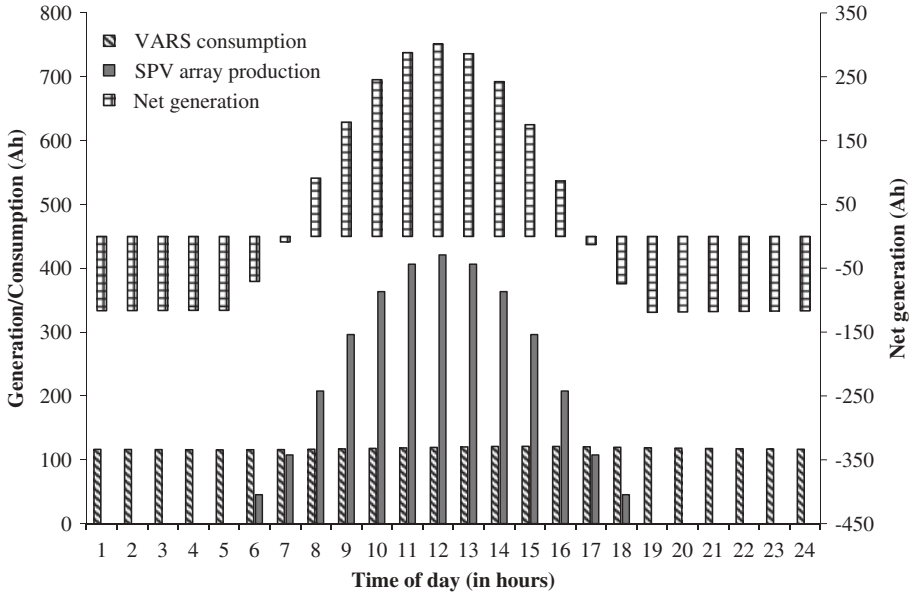

Figure 13. Hourly variation of electrical energy production and consumption by integrated system and net energy flow diagram for a representative day of March.

imum over 12 months owing to very high insolation levels, without much change in the energy consumption levels. Hence, it is possible to have 11 hr of surplus energy production (Figure 14) and net gain in electrical energy is the highest apart from that of the winter months. Month-wise details of energy produced by the SPV array and that consumed by the load over a calendar year are summarized in Table 2. It is found that the largest gain is available in the month of January, while almost insignificant surplus energy is available in the month of October. The designed system produced about 815 Ah of electrical energy per day on an average.

In order to evaluate the cost of running the system with solar energy, a cost analysis is performed for the power system following the methodology detailed earlier. Table 3 shows the size and life-cycle cost of the building integrated system components. It is found that the net present cost for the complete system, including investment required for future batteries, is found to be around US$22,994, leading to an ALCC of about US $1,462 per year. Accordingly, the unit cost of electricity produced by SPV arrays is about INR `7.87 (considering 1 USD ≡ 61 INR) with Energy Payback Time (EBPT) of about 2.7 years.

Conclusions

Present work conceptualizes the use of solar photovoltaic system for powering a H_2O–LiBr absorption system with a cooling load of 3.5 kW for domestic air conditioning in a standalone manner. A mathematical model has been developed, which integrates the absorption system, solar photovoltaic modules, and the storage

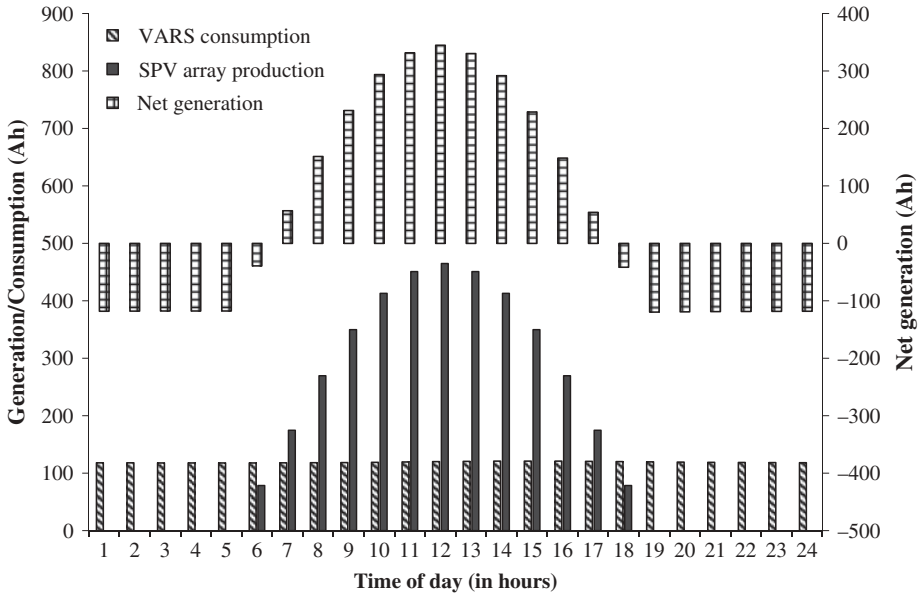

Figure 14. Hourly variation of electrical energy production nd consumption by integrated system and net energy flow diagram for a representative day of June.

Table 2. Details of Energy Production and Consumption for Various Months of a Full Climatic Cycle.

Month	Daily energy production (Ah)	Daily energy consumption (Ah)	Daily energy surplus (Ah)	Monthly energy surplus (Ah)
January	2487.524	1168.012	1319.512	40904.872
February	2831.746	1640.874	1190.872	33344.416
March	3274.025	2830.888	443.137	13737.247
April	3657.273	2863.021	794.252	23827.560
May	3868.248	2866.939	1001.309	31040.579
June	3936.749	2856.917	1079.832	32394.960
July	3868.248	2844.389	1023.859	31739.629
August	3657.273	2844.316	812.957	25201.667
September	3274.025	2844.726	429.299	12878.970
October	2831.746	2831.478	0.268	8.308
November	2487.524	1990.212	497.312	14919.360
December	2377.301	1169.057	1208.244	37455.564
	Surplus energy over a calendar year (Ah)			297453.132
	Average energy surplus per day (Ah)			814.940

Table 3. Size and Life Cycle Cost of Building Integrated PV System Components.

Sl. No.	Component	Size/Rating	Cost (US$)
1	PV array	9750 W_{peak}	47287.50
2	Battery bank	1600 Ah	1600.00
3	Inverter	10725 W	7711.30
4	Charge controller	270.8 A	1589.80
5	Solar power conditioning unit (inverter and charge controller)		9301.10
6	Building integrated PV system cost		58188.60
7	Cost of battery replacement (with 7% rebate on total cost)		1488.00
8	Present battery bank cost		4291.70
9	Net present value (i = 4%)		62480.30
10	Uniform annualized cost		3612.90
11	Annualized life cycle cost (ALCC)		3974.20
	Unit cost of electricity (i = 4%)		0.129

battery. Performance of such a system has been analyzed on a yearly basis. For the proposed operation strategy, the system COP is found to vary 180° out-of-phase with the ambient temperature over a day. The effect of solar radiation intensity on COP of the system, however, is found to be negligible. Variation in the strong and weak solution flow rates conform well to the ambient temperature, while refrigerant flow rate remains almost unaffected throughout the day.

The photovoltaic-based power system for H_2O–LiBr absorption system was also designed. Minimum solar area required for each month of a year was calculated and October was identified as the month demanding the maximum value. It was found that 65 number of CEL make PM-150 modules connected in parallel, along with a battery bank of 1,600 Ah, can successfully meet the power requirements of the system for all the months of a calendar year. Sufficient photovoltaic generation can be observed during high solar insolation periods, which results in considerable surplus energy production during both summer and winter months. Analysis over a full climatic cycle predicts a surplus of about 815 Ah of electrical energy per day on an average. The designed system was also found to be economically viable having per unit electricity cost of INR `7.87 per kWh with energy payback period of about 2.7 years. Present study thus reinforces the viability of a photovoltaic-supported H_2O–LiBr absorption system from both technical and economical point of view, which can be applied for domestic air conditioning and can generate electrical energy to meet the household requirement of the rural community in a standalone manner.

References

Arora, C. P. 2007. *Refrigeration and Air conditioning*. 2nd ed. New Delhi: Tata McGraw Hill.

Asdrubali, F. and S. Grignaffini. 2005. Experimental evaluation of the performances of a H_2O–LiBr absorption refrigerator under different service conditions. *International Journal of Refrigeration* 28(4):489–97.

Best, R. and N. Ortega. 1999. Solar refrigeration and cooling. *Renewable Energy* 16:685–90.

CEL (Central Electronics Limited). 2011. Solar module PM-150 specification. Available online at http://www.celindia.co.in, Accessed on Jan. 12, 2012.

Chel, A., G. N. Tiwari, and A. Chandra. 2009. Simplified method of sizing and life cycle cost assessment of building integrated photovoltaic system. *Energy and Buildings* 41:1172–80.
Chen, G. and E. Hihara. 1999. A new absorption refrigeration cycle using solar energy. *Solar Energy* 66(6):479–82.
Chien, Z.-J., H.-P. Cho, C.-S. Jwo, C.-C. Chien, S.-L. Chen, and Y.-L. Chen. 2013. Experimental investigation on an absorption refrigerator driven by solar cells. *International Journal of Photoenergy* 2013:490124.
Enibe, S. O. 1997. Solar refrigeration for rural applications. *Renewable Energy* 12(2):157–67.
Kim, D. S. and C. A. I. Ferreira. 2008. Solar refrigeration options—a state-of-the-art review. *International Journal of Refrigeration* 31(1):3–15.
Kumar, R. and M. A. Rosen. 2011. A critical review of photovoltaic-thermal solar collectors for air heating. *Applied Energy* 88:3603–14.
Lin, P., R. Z. Wang, and Z. Z. Xia. 2011. Numerical investigation of a two-stage air-cooled absorption refrigeration system for solar cooling: Cycle analysis and absorption cooling performances. *Renewable Energy* 36:1401–12.
Marcos, J. D., M. Izquierdo, and E. Palacios. 2011. New method for COP optimization in water- and air-cooled single and double effect LiBr-water absorption machines. *International Journal of Refrigeration* 34(6):1348–59.
Mastrullo, R. and C. Renno. 2010. A thermo-economic model of a photovoltaic heat pump. *Applied Thermal Engineering* 30(14–15):1959–66.
Moharil, R. M. and P. S. Kulkarni. 2009. A case study of solar photovoltaic power system at Sagardeep Island, India. *Renewable and Sustainable Energy Reviews* 13(3):673–81.
Nawaz, I. and G. N. Tiwari. 2006. Embodied energy analysis of photovoltaic (PV) system based on macro and micro level. *Energy Policy* 34:3144–52.
Patek, J. and J. Klomfar. 2006. A computationally effective formulation of the thermodynamic properties of LiBr–H_2O solutions from 273 to 500 K over full composition range. *International Journal of Refrigeration* 29(4):566–78.
Patra, S. K. and P. P. Datta. 2003. *Some Insights into Solar Photovoltaics–Solar Home Lighting System*. NABARD Technical Digest 7. Mumbai: NABARD. Available online at http://www.nabard.org
Pongtornkulpanich, A., S. Thepa, M. Amornkitbamrung, and C. Butcher. 2008. Experience with fully operational solar driven 10-ton LiBr/H_2O single-effect absorption cooling system in Thailand. *Renewable Energy* 33:943–49.
Razykov, T. M., C. S. Ferekides, D. Morel, E. Stefnakos, H. S. Wall, and H. M. Upadhyaya. 2011. Solar photovoltaic electricity: Current status and future prospects. *Solar Energy* 85:1580–1608.
TEC (Telecommunication Engineering Centre). 2004. *Planning and Maintenance Guidelines for SPV (Solar Photovoltaic) Power Supply*. New Delhi: Telecommunication Engineering Centre. Available online at http://www.tec.gov.in/guidelines.html, Accessed on Jan. 27, 2012.
Tiwari, G. N. 2004. *Solar Energy—Fundamentals, Design, Modeling and Applications*. New Delhi: Narosa.
Tiwari, G. N., R. K. Mishra, and S. C. Solanki. 2011. Photovoltaic modules and their applications: A review on thermal modeling. *Applied Energy* 88(7):2287–2304.
Wagner, W., J. R. Cooper, A. Dittmann, J. Kijima, H.-J. Kretzschmar, A. Kruse, R. Mareš, K. Oguchi, H. Sato, I. Stöcker, O. Šifner, Y. Takaishi, I. Tanishita, J. Trübenbach, and Th. Willkommen. 2000. The IAPWS industrial formulation 1997 for the thermodynamic properties of water and steam. *Journal of Engineering Gas Turbine and Power* 122:150–82.
Zhai, X. Q. and R. J. Wang. 2009. A review for absorption and adsorption solar cooling systems in China. *Renewable and Sustainable Energy Reviews* 13:1523–31.

Nomenclature

A	surface area (m^2)
DF	de-rating factor
C	cost (USD)
$\dot{E}$	power (W)
G	solar radiation intensity (W m^{-2})
h	enthalpy (J kg^{-1})
i	rate of interest
I	current (A)
J	electrical energy (Ah)
$\dot{m}$	mass flow rate (kg s^{-1})
N	number of modules
p	pressure (kg m^{-1} s^{-2})
Q	rate of heat transfer (W)
T	temperature (K)
u_F	air velocity in fan (m s^{-1})
v	specific volume (m^3 kg^{-1})
V_{air}	air flow rate (m^3/s)
V_{system}	system voltage (V)
V_t	module voltage (V)
$\dot{W}$	rate of work transfer (W)
X	mass concentration

Greek symbols

Δp	pressure drop (Pa)
ε	effectiveness
η	efficiency

Subscripts

a	ambient
A	absorber
C	condenser
cc	charge controller
D	diode
des	design
E	evaporator
F	fan
G	generator
in	initial
L	light
m	module
P	pump
p	parallel
PS	power system
r	refrigerant
ref	reference
s	series
sc	short-circuit
ss	strong solution
tot	total
ws	weak solution

Acronyms

Ah	ampere hour
ALCC	annualized life cycle cost
COP	coefficient of performance
EPBT	energy payback time
SPV	solar photovoltaic
VARS	vapor absorption refrigeration system